Reports

Saturn Ring Particles as Dynamic Ephemeral Bodies

Abstract. *Although Saturn's rings are within the Roche zone, the accretion of centimeter-sized particles into large aggregates many meters in diameter occurs readily, on a time scale of weeks. These aggregates are disrupted when tidal stresses exceed their very low strengths; thus most of the mass of the ring system is continually processed through a population of large "dynamic ephemeral bodies," which are continually forming and disintegrating. These large aggregates are not at all like the idealized ice spheres often used in modeling Saturn's ring dynamics. Their coefficient of restitution is low, hence they form a monolayer in the ring plane. The optically observable characteristics of the rings are dominated by the swarm of centimeter-sized particles.*

It has long been understood that Saturn's rings are composed of a myriad of icy particles (*1, 2*), although no individual particle has yet been seen, even by Voyager spacecraft. Those attempting to explain the complex structure of Saturn's rings have invoked continuum properties (for example, viscosity), which actually are the integrated effects of collisions between individual particles. Analytic treatments of ring particle interactions (*3*) are, of necessity, highly idealized, assuming smooth, spherical bodies of uniform size that rebound without any changes in their properties. Here we focus on the details of collisional interactions and their relation to the observed size distribution and inferred physical properties of the ring particles. Consideration of these processes shows that the traditional picture of discrete bodies, maintaining their identities over geological time scales, is qualitatively wrong. Despite the tidal forces within Saturn's Roche zone, ring particles can grow by gravitational accretion. Small particles are quickly incorporated into larger aggregates, which grow until they are disrupted by tidal stresses, whereupon they release the small components to repeat the process. The entire cycle occurs on a time scale of weeks. The dominant ring particles are these ever-changing aggregates or "dynamic ephemeral bodies" (DEB's) (*4*).

During the past decade, it has been recognized that the ring particles have a broad, power-law size distribution (*5, 6*). Optical measurements are most sensitive to the small (centimeter-sized) particles that contribute most of the cross-sectional area. However, the Voyager radio occultation experiment (*7*) revealed that most of the mass of the rings is contained in much larger bodies, typically 3 to 5 m in radius, of which there are $\approx 3000/\text{km}^2$ in the A ring (*8*). We attribute the properties of DEB's to these house-sized bodies. Particles are rather densely packed in the ring system, according to the measured size distribution and the thickness of the rings inferred from analysis of the Voyager 2 stellar occultation data (*9*) and the bending wave excited in the A ring by the satellite Mimas (*10*). The vertical ring thickness of a few tens of meters implies random particle velocities of ≈ 0.1 cm/sec, consistent with Safronov's (*11*) criterion that relative velocities should be of the order of the escape velocity of the bodies of dominant mass. If these parameters for packing density and relative velocity are used, a particle-in-a-box estimate shows that any centimeter-sized ring particle collides with a body having a radius of 3 to 5 m in a few days. If such collisions lead to accretion, large DEB's can form on a time scale of weeks.

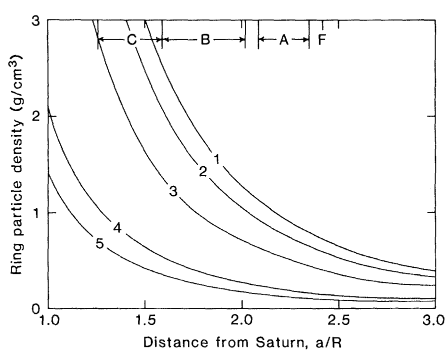

Fig. 1. Critical values of ring particle density, ρ, versus the distance from Saturn, *a*, for phenomena relevant to accretion. Distances are normalized to the mean planetary radius, *R*. All relations are of the form $\rho = C(a/R)^{-3}$, with different values of the coefficient *C*. Curve 1 is the classical Roche limit, $C = 10.37$. Curves 2 through 5 give densities resulting in zero net attraction between two particles in contact with their line of centers in the direction of Saturn (maximum tidal pull). They are as follows: curve 2, equal-sized spheres with synchronous rotation, $C = 8.41$; curve 3, equal spheres, nonrotating, $C = 5.6$; curve 4, a small particle on the surface of a much larger particle, synchronously rotating, $C = 2.09$; and curve 5, a small particle on a much larger, nonrotating particle, $C = 1.40$.

Contrary to popular misconception, accretion is possible at the rings' location within the Roche limit (*4, 12*). The Roche limit is not the distance at which a planet's tidal force exceeds a satellite's gravitational attraction; rather it is the distance inside which no figure of hydrostatic equilibrium exists (*13*). Thus, any solid body within the Roche limit has regions on its surface that are sloped relative to the potential field, but even weak, noncohesive, granular regolith material can maintain an "angle of repose" on the surface of a ring particle and resist the shear stresses. The gravitational force is directed inward everywhere on the surface of a satellite (or ring particle), even well inside the Roche limit, for a wide range of plausible nonhydrostatic shapes (*14*). Whether two contacting ring particles experience a net attraction depends on their relative sizes, shapes, orientation with respect to the tidal field of the planet, rotation rate, and density. The critical density versus distance from Saturn for several limiting cases is shown in Fig. 1.

For sufficiently fast rotation or low density, or both, different parts of the surface of a ring particle can have inwardly and outwardly directed gravity. Although the regions with outward gravity cannot accrete or retain regolith, such material might migrate to other parts of the particle where gravity is inward or perhaps escape completely. Regolith migration may result from the changing orientation of the particle with respect to the planet's tidal forces due to nonsynchronous rotation. By numerical integration of particle motion we have defined conditions under which a small particle will spontaneously escape from the surface of a large ring particle. Outward surface gravity does not guarantee escape; some trajectories return particles to another part of the surface. Thus, large ring particles may be surrounded by swarms of smaller ones in temporary associations. Spontaneous escape is inhibited in the outer part of the rings (where tidal forces are weaker) and for

Table 1. Relevant parameters and regimes for Saturn ring particles of four assumed material types. The mean rotation period depends on density and radius. Other regimes depend on location; C and A refer to location in the C and A ring at 1.38 or 2.10 planetary radii, respectively. A critical period of infinity means that spontaneous escape prevents accretion, even by nonrotating particles.

Density (g/cm^3)	Tensile strength ($dyne/cm^2$)	Coefficient of restitution	Mean rotation period (hours) for a particle diameter of			Critical period for spontaneous escape (hours)		Minimum diameter for accretion (m)		Maximum diameter before tidal disruption	
			1 m	10 m	100 m	C	A	C	A	C	A
						Ice					
0.9	3×10^5	0.25 to 0.5	1.1	11	350	5.5	3.1	0.5	0.3	45 km	85 km
						Snow					
0.2	10^3	0.1	2.4	24	740	∞	12		5	5.5 km	10 km
						Ice assemblage					
0.45	0.01 to 10	0.01	1.6	16	500	∞	5		2.5	12 to 120 m	22 to 220 m
						Snow assemblage					
0.1	0.01 to 10	0.01	3.4	34	1000	∞	∞			25 to 250 m	45 to 450 m

slow rotation. In the A ring, unless rotation periods are $\lesssim$ 3 hours, particles with density $\rho = 0.5$ g/cm^3 are stable against spontaneous leakage.

To our knowledge, there is no direct observational evidence about the spin rates of ring particles. Collisional interactions should dominate over tidal despinning, maintaining nonsynchronous rotation. Applying Harris's treatment (*15*) of the spin evolution of an accreting population with a power-law size distribution, we expect spin periods to be proportional to particle radius r, for $r \lesssim 5$ m. For the reported size distribution (*7*), the spin period (in hours) is predicted to be ~ 0.05 times r (in centimeters); the largest bodies detected by the Voyager radio occultation would, according to this theory, have periods of a few days. Still larger bodies, if they exist, would have spin periods proportional to $r^{3/2}$.

The decrease in spin rate with increasing size predicted by Harris's theory means that spontaneous escape alone cannot limit the accretional growth of the largest ring particles. However, the large aggregates must be disrupted into their component pieces, in order to preserve the observed distribution of centimeter-scale particles that provides most of the visible cross section of the rings. The disruption may be due to tidal stresses, which increase as the square of the particle size (*16*) and must eventually result in material failure. Peak tensile stresses, which would tend to disrupt an aggregate body, generally occur at its surface since the particle's self-gravity places its interior under compression. Tidal stresses overcome interior self-compression only for $\rho < 0.5$ g/cm^3 in the inner B ring or for $\rho < 0.1$ g/cm^3 in the outer A ring. At higher densities, failure of a particle is probably caused by an "avalanche" of a weakened surface layer (*17*).

Table 1 summarizes pertinent bounds on some of the physical processes in the rings. We consider ρ values in the range 0.1 to 0.9 g/cm^3, together with other physical properties characteristic of solid ice, snow, and their aggregates (assemblages with lumps of ice or "snowballs" as building blocks). The mean rotation periods in Table 1 are based on the Harris model and are subject to considerable uncertainty. However, changes in the adopted rotation periods would not alter the basic processes discussed here but would change the minimum diameter for accretion. The tabulated limiting sizes for tidal disruption have little predictive value, since they are based on very uncertain values for tensile strengths, but they indicate that, if tidal disruption is responsible for limiting the growth of DEB's to ~ 10 m, then these strengths must be exceptionally weak. Stresses in particles of this size are only $\sim 10^{-2}$ dyne/cm^2, much less than the strength of solid ice or ordinary cohesive geological materials (10^4 to 10^8 dyne/cm^2), but such low strength may be plausible for aggregates assembled by collisions at very low velocities. In the A ring, particles larger than a few meters can readily grow by accretion unless ρ is $\lesssim 0.1$ g/cm^3. In the C ring only particles with the density of solid ice can begin to accrete, but such accretion forms an aggregate of lower density so that spontaneous escape would begin to inhibit further growth. This difficulty of forming large DEB's in the C ring may help to explain this ring's tenuous nature, if there are mechanisms that tend to remove or destroy small particles.

In order to study the combined effects of the processes described above, we have modified a computer program that we had originally developed to model the collisional evolution of planetesimals and asteroids (*18*). The size distribution of an ensemble of particles is allowed to evolve by collisions, with outcomes including rebound, accretion, and disruption. The modifications to the program introduce effects of tides and spin, including modeling of spontaneous escape and disruption when stress exceeds the assumed strength of the aggregate.

As a test example, we suppressed disruptive processes in order to confirm our particle-in-a-box estimate of accretion rate in the A ring. Using the mechanical properties of solid ice and a coefficient of restitution of 0.25 (*19*), we found that centimeter-sized particles were accreted by bodies larger than 70 cm whereas impacts onto smaller targets resulted in rebound and escape as a result of their lesser gravity. Ignoring disruption by tidal stresses, we found that the larger bodies increased in size by a factor of 10 in only 12 days. That result confirmed the rapid rate of accretion we had earlier estimated.

We then carried out a series of numerical experiments in order to constrain the range of parameters needed to maintain a size distribution similar to that deduced from the Voyager radio occultation data (see Fig. 2). The results depend critically on how we model the effects of tidal disruption. If we consider a large DEB to be tidally split into a few large fragments, then we cannot reproduce the observed size distribution. Virtually all the mass of the system becomes concentrated in a single size interval (near the maximum size) because there is no mechanism for replenishing the population of centimeter-sized particles once they have accreted into DEB's. Alternatively, if we consider a DEB to be tidally split into a shower of small particles, having a power-law size distribution, then the input population quickly evolves to a size distribution similar to the adopted fragmental power law. There are some indications that the real distribution of ring particles has a relative excess of bodies with radii of 3 to 5 m, compared with a simple power-law size distribution (*7*); such a feature can be reproduced if we consider a case intermediate between the two alternatives, with DEB's splitting predominantly into large fragments but with a significant "tail" of smaller particles (*20*). Our models yield equilibrium size distributions (after model times of weeks to months) with features determined chiefly by the adopted mode of tidal splitting.

This result, that the form of the equilibrium size distribution is determined by the assumed size distribution for disruption, is not a general feature of collisional interactions in other contexts (planetesimal growth or asteroid fragmentation). Unfortunately, experiments in terrestrial laboratories cannot physically simulate the tidal breakup of gravitationally bound, cohesionless aggregates. The numerical simulation of Fig. 2 assumes that tidal disruption occurs at $r = 10$ m, corresponding to a tensile strength of only 0.01 dyne/cm^2; whether this is physically reasonable will be difficult to verify experimentally.

Consideration of these critical processes leads to the following conclusions. (i) Small particles are spun up by mutual collisions; because of their rapid rotation and propensity for spontaneous escape, they do not accrete. Meter-sized or larger bodies rotate more slowly, which permits the small particles to accrete onto them to form thick regoliths. These "accretion nuclei" may be remnant solid fragments from primordial times, or they may simply be aggregates. Except in the C ring where accretion is inhibited, the aggregates (DEB's) grow to dimensions of many meters. (ii) Tidal stresses, which increase with size, eventually disrupt the bodies by processes not easily characterized. The dominant mode of disruption may be by an avalanche of loose material from the mantle of a DEB sloughing off in response to the slowly changing orientation of the particle with respect to Saturn's tides as it rotates. Such disruption yields aggregates somewhat smaller than the original body, plus a power-law "tail" of small particles. DEB's may also be destroyed by collisions with other bodies of comparable size, which could mobilize the aggregates and allow tidal forces to disperse them. These processes vary quantitatively from place to place in the rings, but the qualitative picture is everywhere that of a steady-state ensemble of DEB's continually forming and disintegrating on a time scale of days, with a significant population of centimeter-sized constituents shuffling from aggregate to aggregate.

An important conclusion is that monolithic solid ice is an inappropriate model for the ring particles that dominate the system's mass. Dynamical models for the evolution of the ring system (*3*) that relate optical depth to particle collisional velocities must be reconsidered, since they require that the coefficient of restitution be $\gtrsim 0.6$ in order to prevent collapse into a monolayer. However, aggregates or regolith-covered bodies must have much lower coefficients of restitution. Thus, the larger DEB's are arrayed in a monolayer, but their gravitational interactions stir-up centimeter-sized particles into a layer many particles thick, which in fact is not much thicker than the sizes of the larger bodies. This possibility for reconciling optical observational requirements for a distribution that is many particles thick with a dynamic monolayer has been noted by others (*6*). Other interpretations of the ensemble behavior of ring particles (for example, the dependence of effective viscosity on optical depth) may also require reevaluation.

This picture of current ring evolution is consistent with two chief scenarios for the origin of the rings: that they are a primordial remnant of small particles that never accreted into satellites, or that they resulted from the breakup of a large, cohesive satellite (either by tides or collision with another body in either heliocentric or saturnicentric orbit). Our conclusion that centimeter-sized particles do not accrete within the rings might argue against origin from small particles; but, in the absence of larger DEB's the initial relative velocities among the particles would have been much smaller, reducing collisional spin-up and allowing accretion. The satellite breakup model would require extensive collisional processing to yield the present size distribution. In that case, some DEB's might have solid cohesive cores and some larger, cohesive objects may remain in the ring system, conceivably containing sufficient mass to provide a continuing "source" for ring particles. Independent of the underlying size distribution, the aggregation of multimeter DEB's would still occur. Therefore, the measured size distribution may not be diagnostic of mode of origin but may manifest currently operating processes.

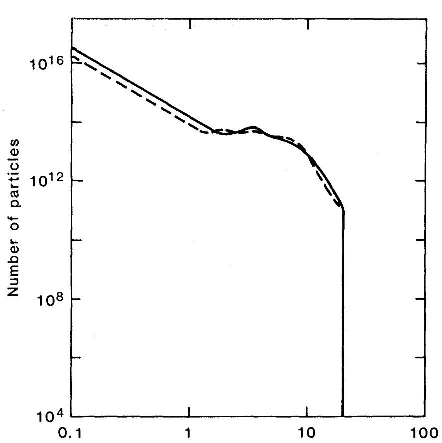

Fig. 2. Example of a numerical investigation of the stability of the particle population of the A ring. The solid line is the input size distribution, chosen to match schematically the principal observed features (*7*): power-law distribution at small sizes, relative excess at r 3 to 5 m, and cutoff at $r \gtrsim 10$ m. Physical parameters are for the ice assemblage, with the strength chosen so that tidal disruption occurs at $r = 10$ m. The dashed line is the distribution after 0.5 year of model time. The close correspondence shows that distributions of this type can result from a steady-state balance of collisional accretion and tidal disruption.

DONALD R. DAVIS
STUART J. WEIDENSCHILLING
CLARK R. CHAPMAN
RICHARD GREENBERG

Planetary Science Institute, Science Applications, Inc., Suite 201, 2030 East Speedway, Tucson, Arizona 85719

References and Notes

1. J. C. Maxwell, *On the Stability of the Motions of Saturn's Rings* (Macmillan, Cambridge, 1859); *Scientific Papers of James Clerk Maxwell* (Cambridge Univ. Press, Cambridge, 1890).
2. Spectroscopic data confirm a composition dominated by frozen H_2O [see C. B. Pilcher, C. R. Chapman, L. A. Lebofsky, H. H. Kieffer, *Science* **167**, 1372 (1970)].
3. P. Goldreich and S. Tremaine, *Icarus* **34**, 227 (1978); G. R. Stewart, D. N. C. Lin, P. Bodenheimer, in *Planetary Rings*, R. Greenberg and A. Brahic, Eds. (Univ. of Arizona Press, Tucson, in press).
4. A more detailed report is in press [S. J. Weidenschilling, C. R. Chapman, D. R. Davis, R. Greenberg, in *Planetary Rings*, R. Greenberg and A. Brahic, Eds. (Univ. of Arizona Press, Tucson, in press)].
5. R. Greenberg, D. R. Davis, W. K. Hartmann, C. R. Chapman, *Icarus* **30**, 769 (1977).
6. J. N. Cuzzi, R. H. Durisen, J. A. Burns, P. Hamill, *ibid.* **38**, 54 (1979).
7. E. A. Marouf, G. L. Tyler, H. Zebker, R. Simpson, V. R. Eshleman, *ibid.* **54**, 189 (1983).
8. It is conceivable that most of the mass of the ring system could reside in bodies ~ 100 m to 1 km in size, dynamically isolated from most other ring particles. Particles of such size could not be detected directly by Voyager and might not have recognizable indirect effects on smaller particles (*4*).
9. A. L. Lane *et al.*, *Science* **215**, 537 (1982).
10. F. H. Shu, J. N. Cuzzi, J. J. Lissauer, *Icarus* **53**, 185 (1983); F. H. Shu, in *Planetary Rings*, R. Greenberg and A. Brahic, Eds. (Univ. of Arizona Press, Tucson, in press).
11. V. S. Safronov, *Evolution of the Protoplanetary Cloud and Formation of Earth and the Planets* (NASA Publication TTF-677, National Aeronautics and Space Administration, Washington, D.C., 1972).
12. R. Smoluchowski, *Nature (London)* **280**, 377 (1979).
13. R. A. Roche, *Academie des Sciences et Lettres de Montpelier, Memoir de la Section des Sci-*

ences **1**, 243 (1847); S. Chandrasekhar, *Ellipsoidal Figures of Equilibrium* (Yale Univ. Press, New Haven, Conn., 1969).
14. A. Dobrovolskis and J. A. Burns, *Icarus* **42**, 422 (1980); D. R. Davis, K. Housen, R. Greenberg, *ibid.* **47**, 220 (1981).
15. A. Harris, *ibid.* **40**, 145 (1979).
16. Rotational stresses are $\sim \rho r^2\omega^2$, tidal stresses are $\sim \rho r^2\Omega^2$, where ω is rotation rate and Ω is orbital frequency; hence, tidal stresses dominate for rotation slower than synchronous.
17. If the "avalanche" involves a substantial fraction of the particle's mass, its own gravitational potential allows easier escape than for the case of a single small particle (*4*).
18. R. Greenberg, J. Wacker, W. Hartmann, C. R. Chapman, *Icarus* **35**, 1 (1978); D. R. Davis, C. R. Chapman, R. Greenberg, S. Weidenschilling, A. Harris, in *Asteroids*, T. Gehrels, Ed. (Univ. of Arizona Press, Tucson, 1979), p. 528.
19. F. Bridges, A. Hatzes, and D. Lin (in preparation) have measured coefficients of restitution of 0.5 to 0.6 for smooth-surfaced ice spheres at the relevant impact speeds of 0.1 cm/sec. Ring particles are unlikely to have such idealized properties; experimental impact studies show that rebound is much slower for slightly irregular or unconsolidated surfaces [W. K. Hartmann, *Icarus* **33**, 50 (1978)]. Even for values of the coefficients of restitution as high as reported by Bridges *et al.*, accretion would occur within Saturn's rings, although at a slower rate than for lower values of the coefficient. Our basic conclusions would be unaffected. Moreover, once some accretion had occurred, the now-unconsolidated surfaces would have low coefficients of restitution.
20. The size distributions of the small and large particles are derived by different methods (*7*). The existence of an excess in the size range from 3 to 5 m is model-dependent; a more recent interpretation by H. Zebker, G. L. Tyler, and E. A. Marouf [*Icarus* **56**, 209 (1983)] suggests that the deviations from a power law are smaller. Nevertheless, most of the mass in the observed size range is in bodies 3 to 5 m in radius. The details of the size distribution do not affect our conclusions.
21. This research was supported by NASA contract NASW-3516. This is Contribution 197 of the Planetary Science Institute, a division of Science Applications, Inc.

6 January 1984; accepted 13 March 1984

Holocene Eruptive Activity of El Chichón Volcano, Chiapas, Mexico

Abstract. *Geologic and radiometric-age data indicate that El Chichón was frequently and violently active during the Holocene, including eruptive episodes about 600, 1250, and 1700 years ago and several undated, older eruptions. These episodes, involving explosive eruptions of sulfur-rich magma and associated dome-growth processes, were apparently separated by intervals of approximately 350 to 650 years. Some of El Chichón's eruptions may correlate with unusual atmospheric phenomena around A.D. 1300 and possibly A.D. 623.*

El Chichón (Fig. 1) erupted violently three times between 28 March and 4 April 1982, causing the worst volcanic disaster in Mexico's recorded history (*1*, *2*). As many as 2000 human lives were lost. Although the recent eruption of El Chichón and that of Mount St. Helens on 18 May 1980 produced roughly equivalent volumes of silicate tephra, El Chichón injected two orders of magnitude more aerosols (10×10^6 to 20×10^6 metric tons) into the lower stratosphere (*3*). The resulting dense volcanic cloud, the atmospheric effects of which are still measurable and being monitored, may affect the weather of the Northern Hemisphere for several years (*3*).

Before the 1982 outburst, El Chichón was an obscure volcano that received little scientific notice since Mullerreid (*4*), in 1928, suggested that its last eruptive activity was in the late Pliocene or early Pleistocene. Several decades later, K-Ar dating (*5*) showed El Chichón to be at least as young as late Pleistocene. Still, with no documentation of historic or late prehistoric eruptions, potential volcanic hazards associated with El Chichón were largely ignored. However, between late 1980 and early 1981, geologists R. Canul and V. Rocha, doing fieldwork in the summit area, frequently heard loud noises and felt earthquakes. In a report (*6*) completed September 1981, they interpreted these phenomena to be related to "subsurface magmatic activity and/or tectonic movements" and warned that "a high volcanic risk" existed at El Chichón. Seven months later the volcano erupted. We describe data showing that the Holocene eruptive history of El Chichón was more eventful than had been supposed. Whether having such information before 1982 might have lent greater urgency to the warning of Canul and Rocha will never be known. Nonetheless, the El Chichón experience underscores the need to document the nature and frequency of a volcano's past eruptions in order to assess the potential for future activity.

Radiometric-age data for El Chichón

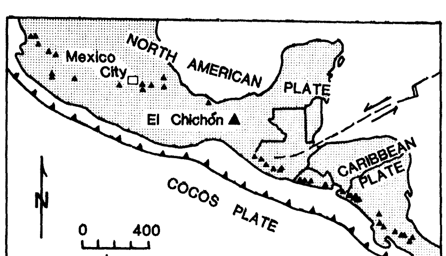

Fig. 1. Index map showing location of El Chichón and generalized tectonic setting of the region. Triangles represent volcanoes.

(Table 1) can be considered in terms of a composite stratigraphic column (Fig. 2). Preliminary studies indicate that all magmatic products are similar in mineralogy and chemistry (*7*). In the interpretation of the radiocarbon ages, we conservatively estimate the overall laboratory variability for a simple measurement to be two or three times the 1 standard deviation (S.D.) counting error (*8*).

The oldest rocks (unit F, Fig. 2) are trachyandesites that make up a 250-m high central dome complex and smaller domes on or near the somma rim (*2*, figure 5). Two samples of dome rock from the eastern somma rim give whole-rock K-Ar ages of 209,000 and 276,000 years before present (B.P.) (Table 1). The rocks of the central dome, destroyed during the 1982 eruptions, have not been dated, but geologic considerations indicate that they are almost certainly younger than the dome rocks dated and probably similar in age to deposits of the pyroclastic unit B (Fig. 2).

The oldest studied pyroclastic deposits (unit E, Fig. 2) are thick debris flows, which rest on domal breccias in the summit area and on Tertiary sedimentary strata elsewhere. They represent block-and-ash flows and other deposits, perhaps generated by (gravitational?) dome collapse, which might be associated with several episodes of dome growth and related explosive activity. Deposits of unit E form the major foundation of the volcano's flanks; no charcoal has yet been found in them.

Next higher in stratigraphic succession is unit D, which rests on a well-developed soil and includes two major pyroclastic flows and associated surge and debris flows. Inasmuch as no major unconformities or soil horizons have been found in unit D, the deposits of this unit were probably emplaced during a single volcanic episode or a series of events in rapid succession. The radiocarbon ages for the upper and middle pyroclastic surge deposits, 1580 and 1600 years B.P., respectively, are consistent with this interpretation.

A duplicate sample from the same horizon as the 1600-year-old sample gave an age of 1870 years B.P.; however, given our estimate of overall laboratory variability (two to three times the 1-S.D. counting error), the difference between these two ages would not be statistically significant. Also, the 1600-year age determination required sample dilution and resulted in the largest error of any of the samples dated (Table 1). A "modern" age for the charcoal collected from the surface of the lower pyroclastic flow of